



Combination of Rainfall Thresholds and Susceptibility Maps for Early Warning Purposes for Shallow Landslides at Regional Scale in Taiwan

An Lu, Wei-Kai Haung, Ching-Fang Lee, Lun-Wei Wei, Hsi-Hung Lin, and Chun-Chi Chi

Abstract

In this study, the development of landslide susceptibility and determination of rainfall threshold for shallow landslides is the main purpose for the prevention of slope disaster. For appliance of the practical operation of disaster prevention, almost 185,000 slope units are used to calculate landslide susceptibility and determine the rainfall threshold of shallow landslides, which are a reference of preparation for slope disasters. Time of occurrence of 941 landslides are collected through field investigation, and rainfall pattern of each landslides are analyzed to clarify the relation between landslide and rainfall. Logistic regression (LR) analysis was performed to evaluate landslide susceptibility and establish the assessment method of the rainfall threshold of landslide by using I_3 - R_{24} rainfall thresholds. After verification of rainfall-induced landslide in Typhoon Meranti (2016), the result show that the early warning model is suitable for alerting serious swarm of landslides.

Keywords

Rainfall-induced landslide • Landslide susceptibility analysis • Rainfall threshold • Early warning

Introduction

Rainfall-induced landslides number among the most perilous natural hazards, causing severe casualties and economic losses worldwide. Therefore, many efforts have been made to evaluate landslide susceptibility and thereby set criteria for issuing alerts that can save lives and property.

In Taiwan, monsoons and typhoons bring great amounts of rainfall, up to 3,000 mm/year, and numerous landslides cause casualties every year. Therefore, recognizing the areas where rainfall-induced landslides might occur is an urgent issue.

On the other hand, rainfall thresholds for landslides can be categorized as either statistical approaches or deterministic approaches. In the former method, thresholds are decided by collecting historical landslide cases and analyzing their rainfall parameters and the probability lines of rainfall conditions (Guzzetti et al. 2008). In the latter method, thresholds are decided by calculating the safety factors of each slope or grid with geomaterial and rainfall parameters (Kim et al. 2010). Statistical rainfall thresholds for shallow landslides have been well discussed (Guzzetti et al. 2007).

This study focused on shallow landslides of the debris fall, debris topples, debris slide, earthfall, earth topple, and earth slide types proposed by Varnes (1978) and divided slope units according to three different landslide susceptibility levels (high, moderate, and low). After that, we established their rainfall thresholds separately. Furthermore, we set alert levels by adopting a hazard matrix and examined whether differentiated warning thresholds for different degrees of susceptibility existed. Moreover, this study gives an importance of validating the performance of a landslide early warning model, especially the false alarms and missed alarms, to make it feasible for further practical application.

A. Lu (✉) · W.-K. Haung · C.-F. Lee · L.-W. Wei
Disaster Prevention Technology Research Center, Sinotech
Engineering Consultants, INC, New Taipei City, Taiwan
e-mail: anlu@sinotech.org.tw

L.-W. Wei
e-mail: lwwei@sinotech.org.tw

H.-H. Lin · C.-C. Chi
Central Geological Survey, MOEA, New Taipei City, Taiwan

Study Area

Taiwan is located in the western Pacific Ocean, on the convergent plate boundary zone of the Philippine Sea Plate and the Eurasian plate. The orogenic uplift rate is 5–7 mm/year; however, the exhumation rate is also as high as 3–6 mm/year (Dadson et al. 2003) due to the fractured geological materials and the high mean annual precipitation of 2,500–3,000 mm brought by typhoons and monsoons every year. The frequent natural disasters and high population density (23 million people in 36,000 km²) of Taiwan make it one of the countries most exposed to multiple hazards.

The study area (Fig. 1) includes 157 1:25,000 scale maps (about 24,250 km²), and covers densely inhabited and landslide-threatening hillslopes. The lithological units are mainly sedimentary rocks composed of sandstone, shale, mudstone, and metamorphic rocks composed of slate, argillite, and metasandstone.

Methodology

Slope Unit

Slope units were used for the analysis of landslide susceptibility in this study (Carrara 1988; Carrara et al. 1991, 1995; Guzzetti et al. 1999; Yang 2017). This study followed the method proposed by Xie et al. (2004) in delineating slope units according to gullies and ridges. Almost 185,000 slope units are found in this study for the establishment of an early warning system.

Landslide Occurrence Time and Field Investigation

To analyze the rainfall conditions for each landslide case used in this study, 941 shallow landslide cases, including their occurrence times (date and hour) and the characteristics of the landslides, were gathered for further analysis.

Landslide Susceptibility Analysis

The main purpose of landslide susceptibility analysis is to determine the effectiveness of each predisposing factor and the relative possibility of landslide occurrence in a specific area.

10 × 10 m DEM is adopted to be a basic resolution for slope unit delineation and landslide susceptibility calculation. Several predisposing factors that might lead to

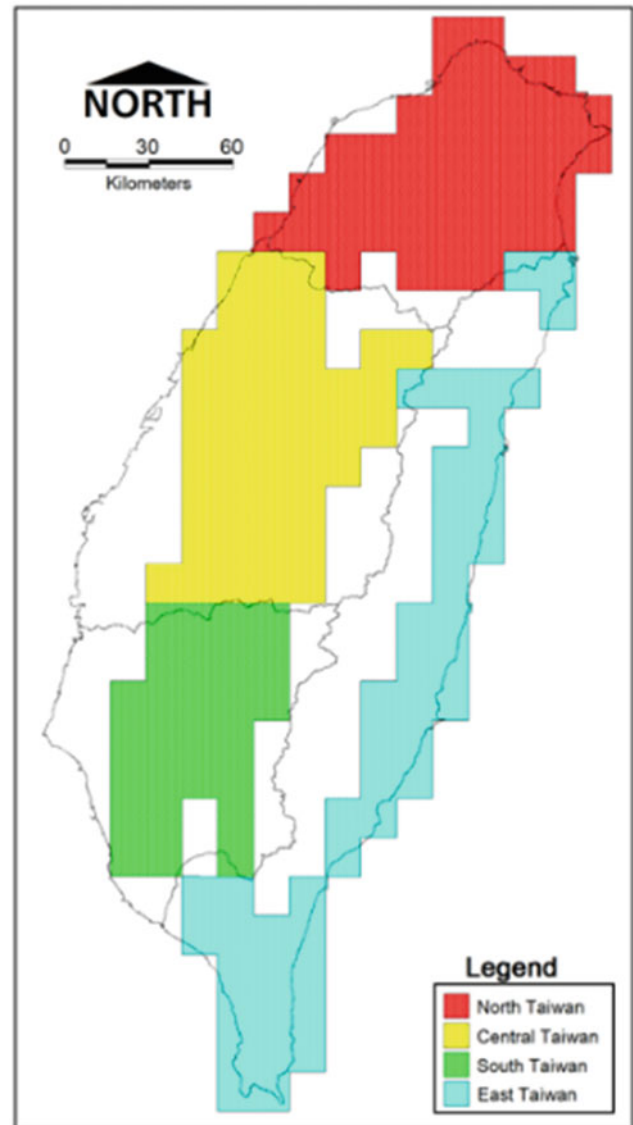


Fig. 1 Study area is composed of 4 regions in Taiwan. Basis of division is different lithological units

landslides were selected initially in this study to construct a landslide susceptibility model for slope units. These factors included rock mass strength-size classification (RMSSC I–VII), dip slope, average slope, variance of slope, ratio of steep slope, total slope height, average elevation, average curvature, variance of curvature, fault density, fold density, average wetness, rainfall intensity, total rainfall, 3-hour mean rainfall intensity (I_3), and 24-hour accumulated rainfall (R_{24}). In this study, we applied logistic regression (LR) to evaluate the susceptibility of each slope unit (Guzzetti et al. 1999). The LR function can be expressed as follows:

$$P = \frac{1}{1 + e^{-z}} \quad (1)$$

$$z = \sum_{i=1}^m L_i w_i + \sum_{j=1}^n F_j w_{m+j} + C \quad (2)$$

where P is landslide susceptibility, L_i is RMSSC factor, F_j is other factors, w_i and w_{m+j} are regression coefficients, and C is a constant. Six event-based landslide inventories in this study were used to label whether or not landslides occurred in the slope units. After that, all the slope units were divided randomly into two groups, one for training the model and the other for validation. The index indicating landslide/non-landslide was set as the dependent variable, and all the landslide susceptibility factors were set as covariates in SPSS for training of the model. After iterative training, the regression coefficients of each landslide susceptibility factor, as well as the success rate curve (SRC), the prediction rate curve (PRC), and the area under the curve (AUC), were reported in SPSS. The AUC can be used to examine if the model predicts landslides well, and the regression coefficients can be used for the prediction of landslide susceptibility. The individual landslide susceptibilities of slope units were calculated with this model and classified into high, moderate and low susceptibility levels.

I_3 – R_{24} Rainfall Index and Thresholds

Rainfall-induced landslides are triggered by either high-intensity rainfall or high accumulated rainfall (Larsen and Simon 1993; Corominas and Moya 1999; Yu et al. 2006). To identify rainfall indexes responsible for landslides, the triggering rainfall, including the rainfall intensity (I_1 , I_2 , I_3 , I_4 , I_5 , I_6) and accumulated rainfall (R_6 , R_{12} , R_{24} , R_{48} , R_{72}) of different time windows of each landslide case were analyzed according to the landslide occurrence time. The results revealed that 218 landslides occurred within the 3 h following the highest rainfall intensity, and 242 occurred within the 3 h following the 2nd or 3rd highest rainfall intensity (i.e., induced by high rainfall intensity), accounting for nearly 49% of the landslide cases gathered in this study. From these results, it became clear that in Taiwan, I_3 is the most important index for landslides induced by rainfall of short duration but high intensity. On the other hand, 481 landslides occurred close to the end of the rainfall events (i.e., induced by high accumulated rainfall), accounting for about 51% of the total cases.

Based on these data and previous studies (Liao et al. 2010), 3-hour mean rainfall intensity (I_3) and 24-hour accumulated rainfall (R_{24}) were chosen respectively as the short-term and long-term rainfall indexes for the establishment of the rainfall threshold (Fig. 2). We chose 3-hour mean rainfall intensity here instead of 3-hour accumulated

rainfall to focus on the rainfall of short duration but high intensity. Similarly, we chose 24-hour accumulated rainfall to focus on the rainfall of long duration but low intensity. Finally, rainfall thresholds were decided by plotting the I_3 and R_{24} rainfall index of historical landslides in the I_3 – R_{24} diagram (Fig. 3). Here we used the ellipse as the threshold line, and the parameters a (semi-major axis) and b (semi-minor axis) of the ellipse were set according to the slope of best fit line obtained from the least square method. Thresholds such as 90, 60, 30 and 15% were determined according to the percentage of historical cases that could be enveloped under the threshold line; e.g., the 90% threshold ($T_{90\%}$) included 90% of the historical cases. A higher threshold indicates a more dangerous condition for the occurrence of landslides. The original warning values of I_3 and R_{24} of the 90, 60, 30, 15% thresholds were equal to the semi-minor axis and semi-major axis of each threshold, respectively. After that, I_3 was rounded to the nearest 5 mm/h, and R_{24} was rounded to the nearest 50 mm for operational purposes, such as the evacuation of residents.

Landslide Early Warning Model

The landslide early warning model in this study considered both landslide susceptibility and rainfall thresholds and alerts were determined by using a hazard matrix. As mentioned above, the LR method was applied to analyze the susceptibility of each slope unit. After that, all the slope units were categorized into high, moderate, and low susceptibility levels. We consequently established rainfall thresholds for each susceptibility level separately and then set alerts of red, orange, yellow and green according to the level of danger.

High-susceptibility slopes might be more susceptible to rainfall. Hence, the alerts were set as red (extreme danger level) for rainfall conditions exceeding the 60% threshold line, orange (high danger level) for those between the 60 and 30% threshold lines, yellow (medium danger level) for those between the 30 and 15% threshold lines, and green (low danger level) for rainfall conditions lower than the 15% threshold line (Fig. 4). For moderate-susceptibility slopes, the alerts were set as red for rainfall conditions exceeding the 90% threshold line, orange for those between the 90 and 60% threshold lines, yellow for rainfall conditions between the 60 and 30% threshold lines, and green for rainfall conditions lower than the 30% threshold line. Low-susceptibility slopes should be less susceptible to rainfall. Hence, the alerts were set as orange for rainfall conditions exceeding the 90% threshold line, yellow for those were between 90 and 60% threshold lines, and green for those lower than the 60% threshold line (Fig. 5).

Fig. 2 3-hour mean rainfall intensity (I_3) and 24-hour accumulated rainfall (R_{24}) were used as short-term and long-term rainfall indexes for the establishment of rainfall thresholds

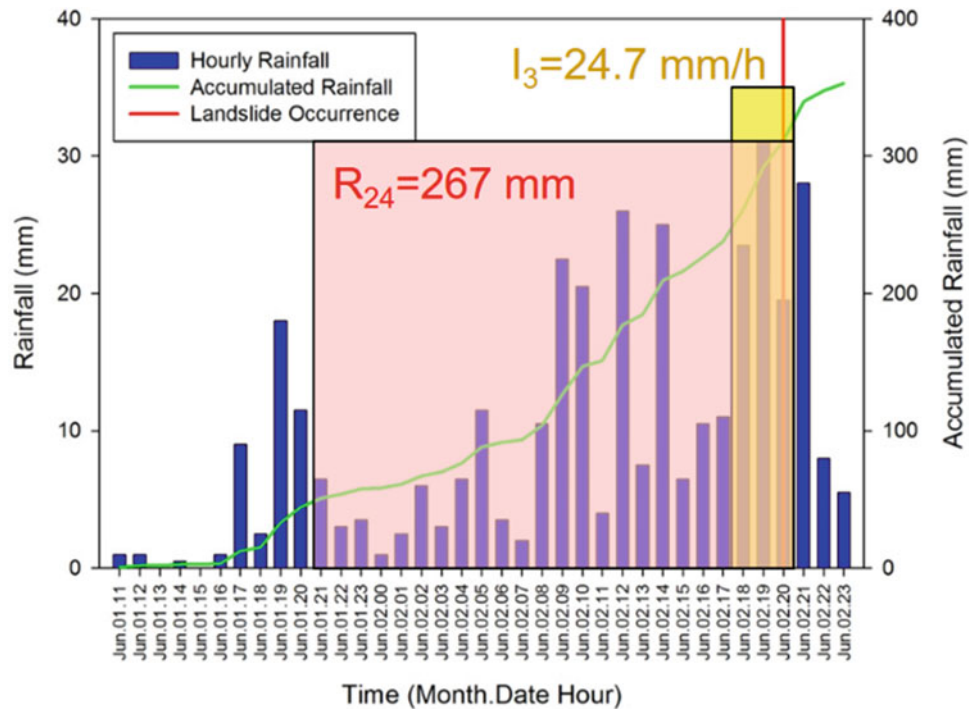
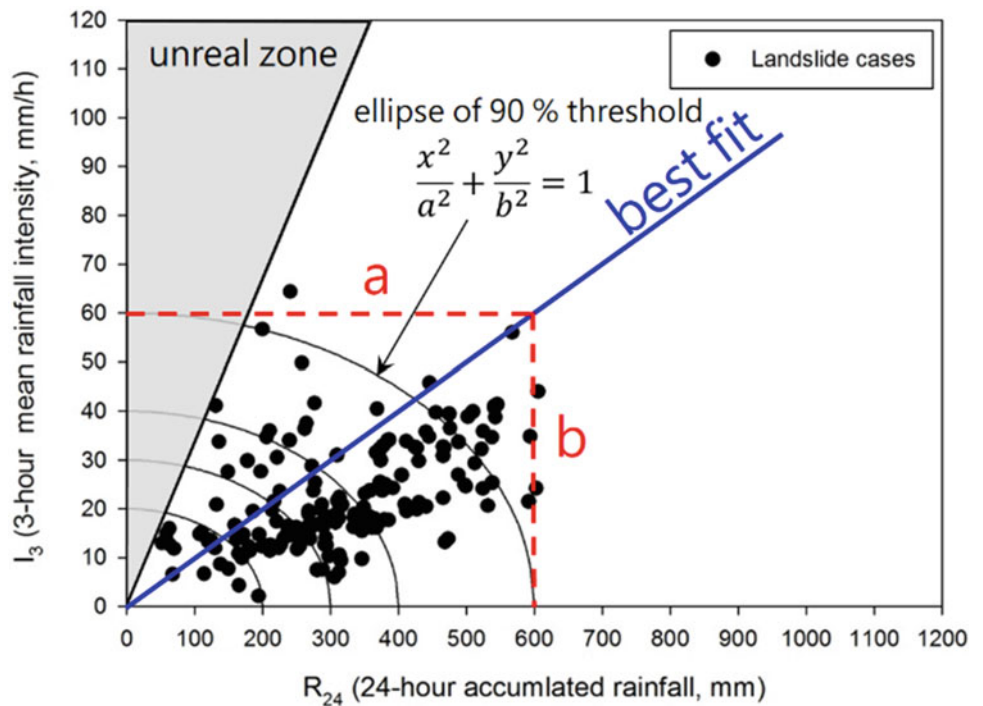


Fig. 3 Establishment of I_3 - R_{24} rainfall thresholds for shallow landslides. The best fit line was derived by the least square method, and the ratio of a and b was used as the ratio of the semi-major axis and semi-minor axis in the ellipse threshold line



I_3 - R_{24} Rainfall Threshold

We gathered a total of 941 landslide cases in this study and used 240 cases located in southern Taiwan, consisting of 110 high-susceptibility cases, 84 moderate-susceptibility cases,

and 46 low-susceptibility cases, to establish a susceptibility-based regional landslide early warning model. For practical use, the original threshold values of I_3 and R_{24} (as shown in the parentheses in Fig. 6) were separately rounded to the nearest 5 mm/h and the nearest 50 mm for an operational purpose. It was found that the threshold values gradually

Fig. 4 Landslide early warning model and alert considering both landslide susceptibility and rainfall thresholds

		Rainfall threshold (T)							
		T _{90%}		T _{60%}		T _{30%}		T _{15%}	
		I ₃	R ₂₄	I ₃	R ₂₄	I ₃	R ₂₄	I ₃	R ₂₄
Landslide susceptibility	High susceptibility	Extreme danger level		Extreme danger level		High danger level		Medium danger level	
	Moderate susceptibility	Extreme danger level		High danger level		Medium danger level		Low danger level	
	Low susceptibility	High danger level		Medium danger level		Low danger level		Low danger level	

Fig. 5 Rainfall thresholds for southern Taiwan. The values were calculated as 90, 60, 30, and 15% of the original threshold, respectively. The original values are shown in parentheses

		Rainfall threshold (T)							
		T _{90%}		T _{60%}		T _{30%}		T _{15%}	
		I ₃	R ₂₄	I ₃	R ₂₄	I ₃	R ₂₄	I ₃	R ₂₄
Landslide susceptibility	High susceptibility	70 (68)	750 (745)	55 (56)	600 (610)	40 (40)	450 (438)	30 (27)	300 (291)
	Moderate susceptibility	70 (61)	650 (657)	45 (46)	500 (498)	35 (34)	350 (368)	20 (22)	250 (236)
	Low susceptibility	50 (50)	550 (539)	40 (40)	450 (430)	30 (29)	300 (316)	15 (15)	200 (167)

increased as the susceptibility of slope units decreased for the same alert level, indicating that greater rainfall amounts would be needed when issuing alters on less susceptible slope units. These results showed that establishing rainfall thresholds

according to different landslide susceptibilities and then setting alert levels by adopting a hazard matrix provided differentiated not only thresholds but also avoided the over- or underestimation of the thresholds for slopes.

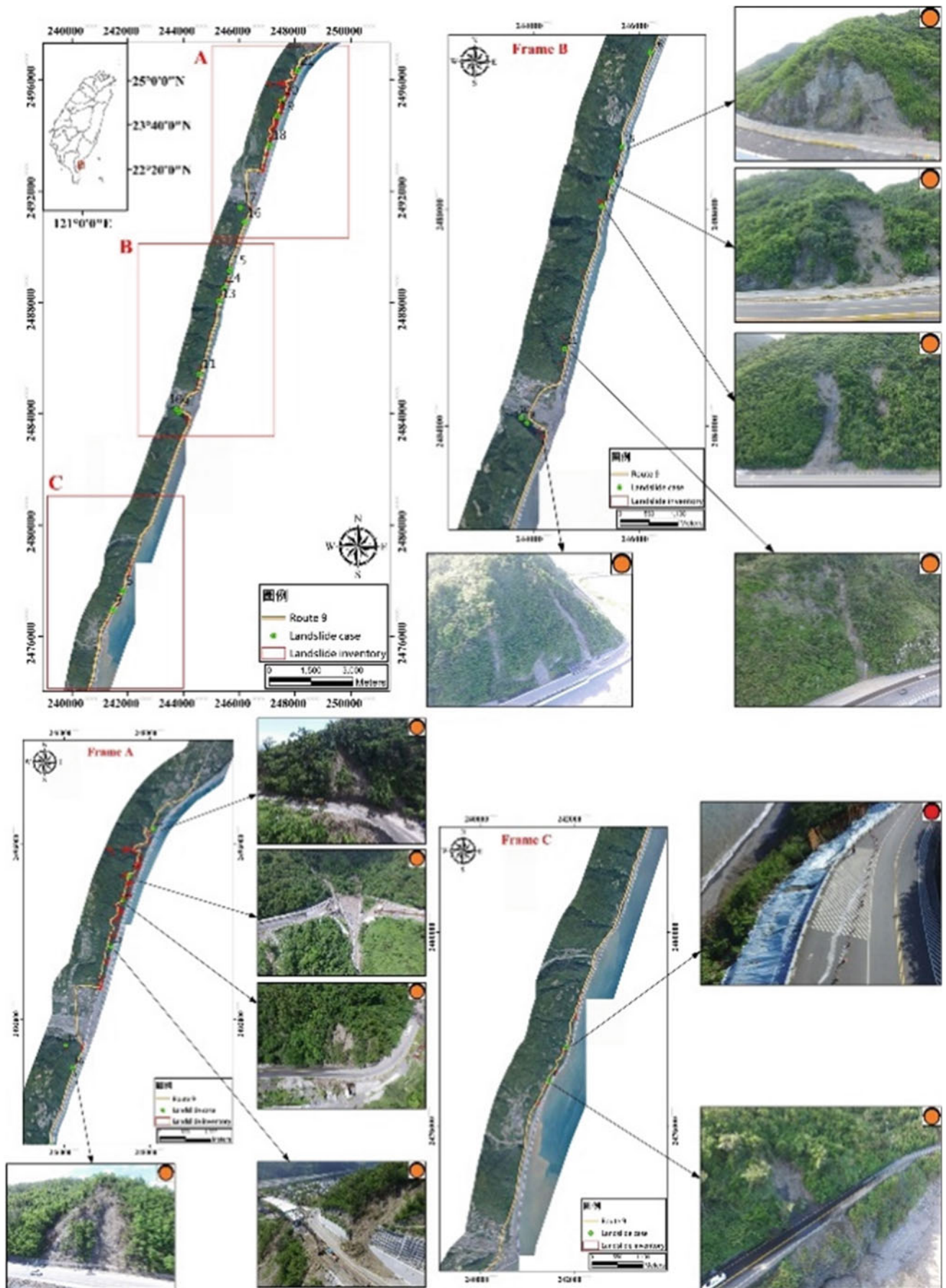
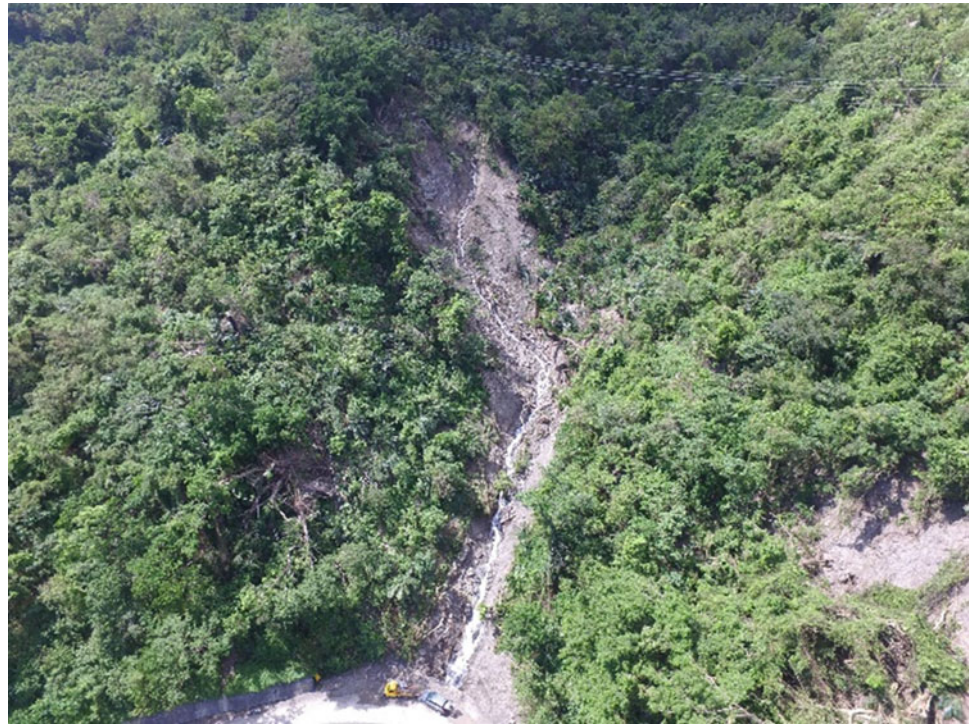


Fig. 6 Location and alert level of 12 representative landslides near route 9 caused by Typhoon Meranti in 2016

Fig. 7 Photo of route 9 410.8 k landslide



Validation of Early Warning Model

During Typhoon Meranti in 2016, 178 shallow landslides occurred in 29 slope units, including one high-susceptibility slope, two moderate-susceptibility slopes, and 26 low-susceptibility slopes. According to newspaper reports, most of the landslides occurred at 04:00 on September 15, 2016. Alert level and photo of 12 shallow landslides, which are representative from 178 shallow landslides, are shown in Fig. 7. One of them was a red alert level when the landslide occurred; the others are orange alert level.

The Route 9 410.8 k landslide (Fig. 8) occurred on a low-susceptibility slope in southern Taiwan. The rainfall path (Fig. 9) showed that on September 15, the alert was raised to yellow at 02:00. Then the landslide occurred at 05:00 on September 15. The Route 9 413.5 k landslide (Fig. 10) occurred on a low-susceptibility slope in southern Taiwan. The rainfall path (Fig. 10) showed that on September 15, the alert was raised to yellow at 00:00 and then to orange at 02:00 during the downpour. Then the landslide occurred at 04:00 on September 15.

Conclusion

This study attempted to establish regional rainfall thresholds for shallow landslides according to their landslide susceptibility levels and set alerts with a hazard matrix to provide more detailed results for disaster mitigation.

This study also examined the relationships between rainfall indexes and the occurrence of landslides. From 941 landslide cases we gathered, it was found that 3-hour mean rainfall intensity (I_3) and 24-hour accumulated rainfall (R_{24}) was the most dominant short-term and long-term parameters responsible for rainfall-induced landslides in Taiwan. There were 460 cases (about 49%) that occurred within the 3 h following the highest, 2nd, and 3rd rainfall intensities, while 24-hour accumulated rainfall had the lowest coefficient of variation of the long-term rainfall indexes. The I_3 - R_{24} rainfall index was therefore used to establish rainfall thresholds.

Slope units are categorized into three landslide susceptibility levels (high, moderate, and low) and then separately established a susceptibility-based regional rainfall threshold.

Fig. 8 Rainfall path of route 9 410.8 k landslide in the I_3 - R_{24} diagram

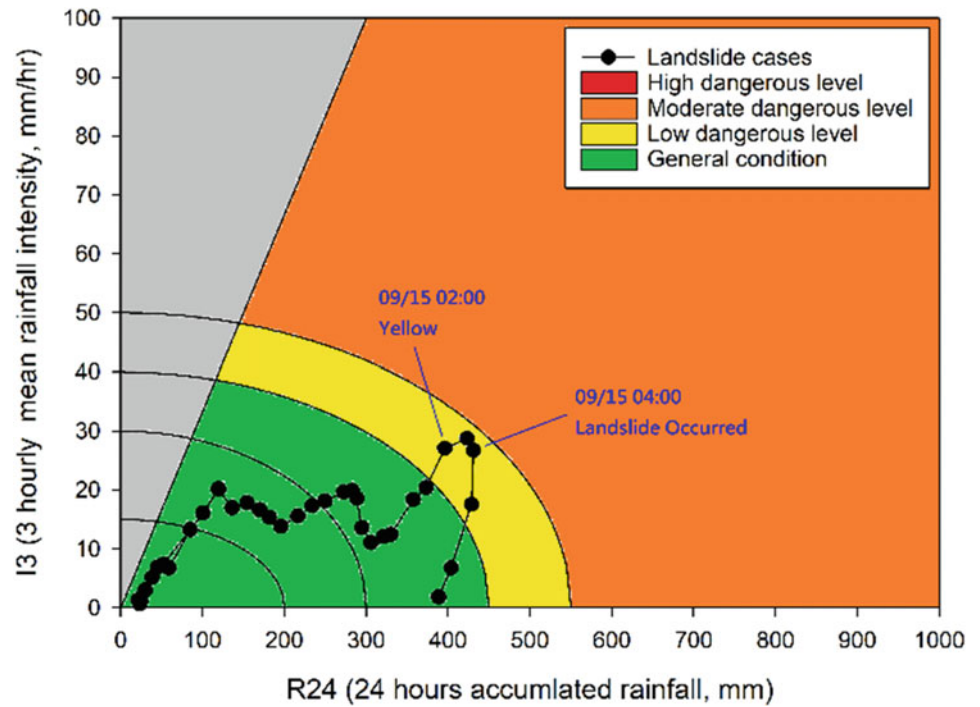


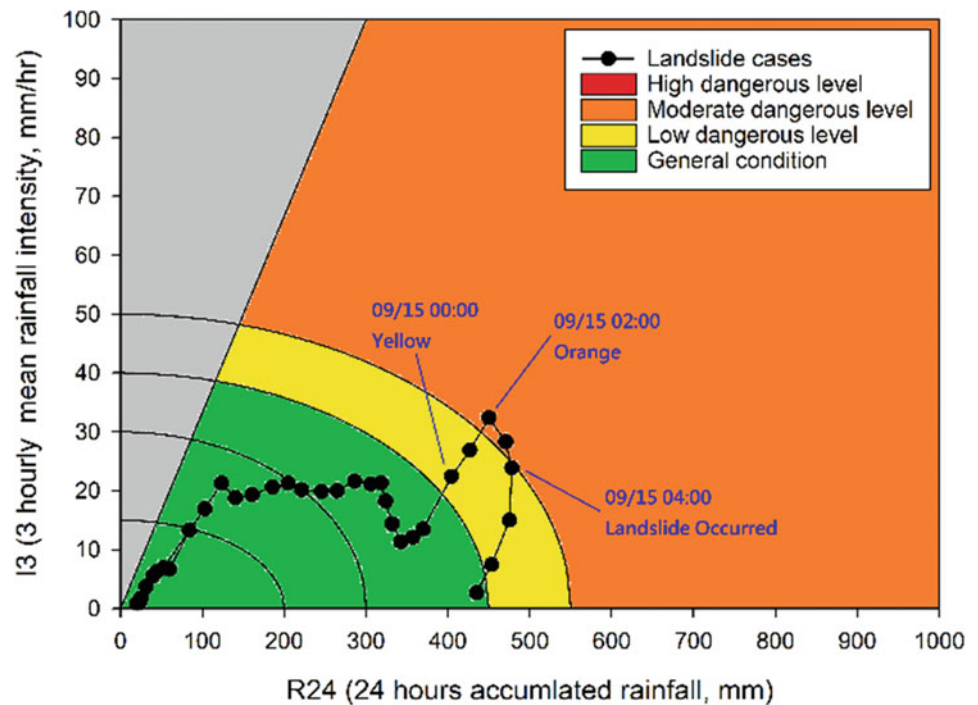
Fig. 9 Photo of route 9 413.5 k landslide



We also set three alert levels, including red (extreme danger level), orange (high danger level), and yellow (medium danger level), by adopting a hazard matrix for application to evacuation decisions.

Validations using landslide cases in Typhoon Meranti in 2016 showed that, for the representative landslide cases in Typhoon Meranti, orange or red alerts could have been issued before the landslides occurred.

Fig. 10 Rainfall path of route 9 413.5 k landslide in the I_3 - R_{24} diagram



It can be concluded that classifying landslide susceptibility and establishing rainfall thresholds separately not only provides refined thresholds but also avoids over- or under-estimation of the thresholds for slopes, especially when considering the application to disaster prevention.

Acknowledgements The authors would like to thank the Central Geological Survey, Taiwan, for supporting this research financially and for providing helpful comments on the research.

References

- Carrara A (1988) Quantitative analysis of mineral and energy resources. Springer, Dordrecht, pp 581–597
- Carrara A, Cardinali M, Detti R, Guzzetti F, Pasqui V, Reichenbach P (1991) GIS techniques and statistical models in evaluating landslide hazard. *Earth Surf Proc Land* 16(5):427–445
- Carrara A, Guzzetti F (1995) Geographical information systems in assessing natural hazards. Springer, Netherlands, pp 135p–175p
- Corominas J, Moya J (1999) Reconstructing recent landslide activity in relation to rainfall in the Llobregat River basin, Eastern Pyrenees. *Spain Geomorphol* 30(1):79–93
- Dadson SJ, Hovius N, Chen H, Dade WB, Hsieh ML, Willett SD, Hu JC, Horng MJ, Chen MC, Stark CP, Lague D, Lin JC (2003) Links between erosion, runoff variability and seismicity in the Taiwan orogeny. *Nature* 426(6967):648–651
- Guzzetti F, Carrara A, Cardinali M, Reichenbach P (1999) Landslide hazard evaluation: a review of current techniques and their application in a multi-scale study. *Central Italy Geomorphol* 31(1):181–216
- Guzzetti F, Peruccacci S, Rossi M, Stark CP (2007) Rainfall thresholds for the initiation of landslides in central and southern Europe. *Meteorol Atmos Phys* 98(3–4):239–267
- Guzzetti F, Peruccacci S, Rossi M, Stark CP (2008) The rainfall intensity-duration control of shallow landslides and debris flows: an update. *Landslides* 5(1):3–17
- Kim D, Im S, Lee SH, Hong Y, Cha KS (2010) Predicting the rainfall-triggered landslides in a forested mountain region using TRIGRS model. *J Mt Sci* 7(1):83–91
- Larsen MC, Simon A (1993) A rainfall intensity-duration threshold for landslides in a humid-tropical environment, Puerto Rico. *Geogr Ann Series A, Phys Geogr.* 75:13–23
- Liao Z, Hong Y, Wang J, Fukuoka H, Sassa K, Karnawati D, Fathani F (2010) Prototyping an experimental early warning system for rainfall-induced landslides in Indonesia using satellite remote sensing and geospatial datasets. *Landslides.* 7(3):317–324
- Xie M, Esaki T, Zhou G (2004) GIS-based probabilistic mapping of landslide hazard using a three-dimensional deterministic model. *Nat Hazards* 33(2):265–282
- Yang SR (2017) Assessment of rainfall-induced landslide susceptibility Using GIS-based slope unit approach. *J Perform Constr Fac* 31(4):04017026
- Yu FC, Chen TC, Lin ML, Chen CY, Yu WH (2006) Landslides and rainfall characteristics analysis in Taipei City during the Typhoon Nari event. *Nat Hazards* 37(1):153–167